The Astrophysical Journal, 817:90 (11pp), 2016 February 1 doi:10.3847/0004-637X/817/2/90


# BREEDING SUPER-EARTHS AND BIRTHING SUPER-PUFFS IN TRANSITIONAL DISKS

Eve J. Lee[1] and Eugene Chiang[1,2]
[1] Department of Astronomy, University of California Berkeley, Berkeley, CA 94720-3411, USA; evelee@berkeley.edu, echiang@astro.berkeley.edu
[2] Department of Earth and Planetary Science, University of California Berkeley, Berkeley, CA 94720-4767, USA
*Received 2015 September 2; accepted 2015 November 23; published 2016 January 22*

## ABSTRACT

The riddle posed by super-Earths (1–4$R_\oplus$, 2–20$M_\oplus$) is that they are not Jupiters: their core masses are large enough to trigger runaway gas accretion, yet somehow super-Earths accreted atmospheres that weigh only a few percent of their total mass. We show that this puzzle is solved if super-Earths formed late, as the last vestiges of their parent gas disks were about to clear. This scenario would seem to present fine-tuning problems, but we show that there are none. Ambient gas densities can span many (in one case up to 9) orders of magnitude, and super-Earths can still robustly emerge after ∼0.1–1 Myr with percent-by-weight atmospheres. Super-Earth cores are naturally bred in gas-poor environments where gas dynamical friction has weakened sufficiently to allow constituent protocores to gravitationally stir one another and merge. So little gas is present at the time of core assembly that cores hardly migrate by disk torques: formation of super-Earths can be in situ. The basic picture—that close-in super-Earths form in a gas-poor (but not gas-empty) inner disk, fed continuously by gas that bleeds inward from a more massive outer disk—recalls the largely evacuated but still accreting inner cavities of transitional protoplanetary disks. We also address the inverse problem presented by super-puffs: an uncommon class of short-period planets seemingly too voluminous for their small masses (4–10$R_\oplus$, 2–6$M_\oplus$). Super-puffs most easily acquire their thick atmospheres as dust-free, rapidly cooling worlds outside ∼1 AU where nebular gas is colder, less dense, and therefore less opaque. Unlike super-Earths, which can form in situ, super-puffs probably migrated in to their current orbits; they are expected to form the outer links of mean-motion resonant chains, and to exhibit greater water content. We close by confronting observations and itemizing remaining questions.

*Key words:* planets and satellites: atmospheres – planets and satellites: formation

## 1. INTRODUCTION

The *Kepler* spacecraft has established that about half of all Sun-like stars harbor at least one planet (e.g., Fressin et al. 2013). Of these, the most common are "super-Earths," here defined as those objects having radii between 1 and 4 $R_\oplus$. Super-Earths are found orbiting ∼60% of FGK-type dwarfs with periods $< 85$ days (Howard et al. 2010; Batalha et al. 2013; Dong & Zhu 2013; Fressin et al. 2013; Petigura et al. 2013; Rowe et al. 2014). Transit-timing analyses (Wu & Lithwick 2013) and radial velocity surveys (Weiss & Marcy 2014) have determined that the typical masses of super-Earths are ∼2–20 $M_\oplus$. These masses overlap with the range of core masses believed to trigger the formation of gas giants, according to the theory of core-nucleated instability (e.g., Mizuno 1980, Stevenson 1982, Pollack et al. 1996, Ikoma et al. 2000). Yet super-Earths are not Jupiters; the gas-to-core mass ratios (GCRs) of super-Earths are of order 1%–10% (e.g., Rogers & Seager 2010a, 2010b; Lopez & Fortney 2014). They are too small to be gas giants and too large to be purely rocky.[3]

Motivated by these discoveries, we have investigated in a series of papers the physics of nebular accretion: how rocky cores at stellocentric distances of 0.1–5 AU acquire gas from their parent nebulae (Lee et al. 2014, hereafter Paper I; Lee & Chiang 2015, hereafter Paper II). The rate at which planets siphon gas from their natal disks is limited by how fast such gas can cool. As atmospheres cool, they shrink, allowing nebular gas to refill the planets' Hill (or Bondi) spheres. Atmospheric cooling is regulated by the thermodynamic properties of radiative-convective boundaries (rcb's). In dusty atmospheres, rcb properties are set by the microphysics of dust sublimation and $H_2$ dissociation, not by external nebular conditions. Regardless of their orbital distance, dusty atmospheres atop cores of mass $\gtrsim 5\ M_\oplus$ undergo runaway gas accretion to spawn Jupiters, when embedded in gas-rich disks (Paper I).[4] Dust-free atmospheres have rcb's that do depend on nebular environment; nevertheless, because they generally cool faster than dusty atmospheres, they are also prone to gravitational collapse essentially everywhere in protoplanetary nebulae (Paper II). The threat of runaway is all the more serious because it cannot be neutralized by heating from infalling planetesimals; such heating tends to be overwhelmed by the acceleration of gas accretion from increasing core mass (Paper II).

Paper I proposed two ways to circumvent runaway. In scenario (a), super-Earths can stay as super-Earths, even in gas-rich nebulae, provided their atmospheres are chock-full of dust. Supersolar dust-to-gas ratios render atmospheres so opaque that their cooling times exceed the nebular lifetime. This scenario finds empirical support in the supersolar metallicities of observed super-Earth atmospheres (e.g., Morley et al. 2013; Knutson et al. 2014; Kreidberg et al. 2014). In scenario (b), super-Earth cores did not nucleate Jupiters simply because they

[3] Structurally they most resemble Neptune ($4R_\oplus$, $17M_\oplus$, GCR $\simeq$ 10%), prompting some to call them "mini-Neptunes" or "sub-Neptunes." We will stick to "super-Earths."

[4] "Runaway" ensues when the atmospheric mass becomes comparable to the core mass: when the self-gravity of the gas envelope strongly enhances the cooling rate. Runaway is a thermodynamic catastrophe, not a dynamic one; the envelope remains hydrostatic throughout. To maintain hydrostatic equilibrium as the envelope's self-gravity grows, the cooling luminosity rises dramatically, hastening the cooling and contraction of the envelope and thereby causing the Hill (or Bondi) sphere to refill at a faster rate. This positive feedback loop between self-gravity, cooling, and accretion causes the planet to balloon into a gas giant.

were born at the tail end of the gas disk's life, with only dregs of gas remaining for ∼1 Myr or so. The formation of cores from smaller mass protocores is arguably delayed until disk gas is largely depleted: only then is gas dynamical friction weak enough to permit protocores to gravitationally stir each other, cross orbits, and merge (see, e.g., Dawson et al. 2015a).

In the present paper, we revisit these two proposed formation pathways for super-Earth atmospheres. In Sections 2 and 3, respectively, we re-examine scenarios (a) and (b), more critically assessing their strengths and weaknesses to decide whether a gas-rich or gas-poor formation environment is more likely. A concern common to both scenarios is that fine-tuning of parameters is needed to obtain desired outcomes. We will confront this concern head-on.

The conundrum of super-Earths is that many of them have too little gas for their large core masses. The flip side of this puzzle is presented by "super-puffs": a rare class of *Kepler* planets characterized by orbital periods $\lesssim$ 50 days, radii ∼4–10 $R_\oplus$, masses ∼2–6 $M_\oplus$, and inferred GCRs $\gtrsim$ 20% (e.g., Lopez & Fortney 2014; Masuda 2014). Super-puffs seem to have too much gas for their small core masses. To attain their large GCRs, super-puff cores must have enjoyed an environment that enabled rapid atmospheric cooling. In Section 4, we show how such an environment obtains at large stellocentric distances, outside ∼1 AU—thus implicating orbital migration for the origin of super-puffs.

Our series of three papers studies how planetary atmospheres are built from nebular accretion, with the ultimate goal of explaining how super-Earths and super-puffs got their gas. The solutions we provide inspire new questions and point to future areas of improvement, as well as ways in which our ideas can be tested by observers. We attempt to provide this "big-picture" view in Section 5, where we summarize our results and chart the way forward.

All calculations of nebular accretion throughout this paper derive from the numerical models of passively cooling atmospheres of Paper I, or their analytic counterparts in Paper II. Readers interested in the underlying machinery should consult those studies. We have tried to write this third paper so that it can be understood with as few technical references as possible, relegating such information mostly to figure captions.

## 2. DANGERS OF RUNAWAY IN GAS-RICH, METAL-RICH NEBULAE (SCENARIO A)

Increasing the dust content—and by extension the metallicity—of nebular gas increases the opacity of the accreted atmosphere. Dustier atmospheres cool more slowly, accrete less efficiently, and are thus less prone to runaway (e.g., Stevenson 1982; Ikoma et al. 2000; Piso & Youdin 2014; Paper I; Piso et al. 2015). High metallicities for super-Earth atmospheres are also motivated by observations: the notoriously flat transmission spectra of GJ 3470b, GJ 1214b, and GJ 436b can be attributed to clouds or hazes that form only in environments with supersolar metallicities (e.g., ∼50 × solar; Crossfield et al. 2013; Morley et al. 2013; Biddle et al. 2014; Knutson et al. 2014; Kreidberg et al. 2014). The atmosphere of HAT-P-11b may have patchy clouds (Line & Parmentier 2015) or be cloud-free; the latter interpretation still implicates a supersolar metallicity ($Z \gtrsim 0.6$), as judged from the planet's water absorption feature (Fraine et al. 2014, their Figures 2 and 3).

If the effects of raising the dust-to-gas ratio were limited to increasing the opacity, then high atmospheric metallicities could explain how super-Earths avoided runaway even in gas-rich nebulae. Life, unfortunately, is not so simple. We can identify two reasons why dust/metal enrichment may not save super-Earths from exploding into Jupiters, in disks with full complements of gas:

1. High metallicity gas has high mean molecular weight and is therefore more susceptible to gravitational collapse (e.g., Hori & Ikoma 2011; Nettelmann et al. 2011; Paper II).
2. Grains can coagulate and sediment out of radiative layers, forfeiting their contributions to the opacity (e.g., Mordasini et al. 2014; Ormel 2014).

We quantify these weaknesses below.

Throughout this paper, our proxy for a gas-rich disk is the "minimum-mass extrasolar nebula" (MMEN) of Chiang & Laughlin (2013): a solar-composition disk having enough solid material to form *Kepler*-like systems. Its gas surface density is $\Sigma_{\rm MMEN} = 4 \times 10^5\,(a/0.1\,{\rm AU})^{-1.6}\,{\rm g\,cm^{-2}}$, which is about 5× larger than that of the conventional minimum-mass solar nebula. The assumed temperature profile is $T_{\rm MMEN} = 1000\,(a/0.1\,{\rm AU})^{-3/7}\,{\rm K}$, and the volumetric gas density is $\rho_{\rm MMEN} = 6 \times 10^{-6}\,(a/0.1\,{\rm AU})^{-2.9}\,{\rm g\,cm^{-3}}$. "Dusty" models assume a relative grain size distribution similar to that of the diffuse interstellar medium (Ferguson et al. 2005), while "dust-free" models take all metals to be in the gas phase at their full assumed abundances.

### 2.1. High-μ Catastrophe

Metal enrichment breeds atmospheres with high mean molecular weight $\mu$. Such atmospheres more easily collapse under their own weight, triggering the formation of gas giants. Figure 1 illustrates the danger of having too high a metallicity $Z$. As $Z$ increases from 0.02 to 0.2, the critical core mass $M_{\rm crit,core}$ for runaway gas accretion—evaluated at 0.1 AU in a dusty MMEN—increases from 5 to 8 $M_\oplus$ as rising opacities impede cooling and accretion. But further gains in $M_{\rm crit,core}$ with $Z$ are not to be had; for $Z \gtrsim 0.2$, enhancements in opacity are outweighed by increases in $\mu$. The critical core mass stays at about 5–6$M_\oplus$ for $Z = 0.5$–$0.6$ ($\mu \simeq 4$), and drops to as low as 2 $M_\oplus$ for $Z = 0.8$ ($\mu \simeq 7.5$).[5] Here we define the critical core mass such that its runaway time (when the atmospheric cooling luminosity attains a minimum; see Papers I and II) equals the total disk lifetime of ∼10 Myr (Mamajek 2009; Alexander et al. 2014).

The similarity of the critical core masses plotted in Figure 1 to observed super-Earth masses (e.g., Weiss & Marcy 2014) is a primary reason for believing that super-Earths did not form in a gas-rich disk. At no metallicity is a 10 $M_\oplus$ core embedded in an undepleted nebula able to remain a super-Earth. We shall see in the next section that even the modest advantage presented by a 10–20× dust-enhanced disk in staving off runaway may be erased by grain growth.

[5] Critical core masses can decrease even further because increasing $Z$ increases the potential for molecular chemistry and phase changes, both of which consume energy and render gas more isothermal, steepening density gradients. These effects are more significant at larger orbital distances where gas is colder and hosts more molecules; see Section 4 for more details.

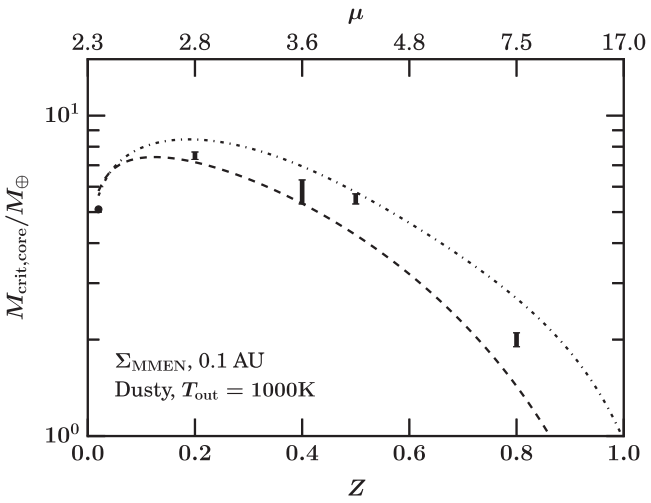


**Figure 1.** Critical core masses $M_{\rm crit,core}$ do not rise monotonically with dust-to-gas ratio $Z$. For $Z \gtrsim 0.2$, atmospheres are actually more susceptible to runaway because of the increasing molecular weight $\mu$ (top axis). Results are calculated for dusty atmospheres at 0.1 AU in the "gas-rich" MMEN. The lower limit on each error bar is the maximum $M_{\rm core}$ that can be numerically evolved; for $Z = 0.02$–$0.8$, their runaway times (when planetary luminosities reach their minima and start increasing) are 10.5, 11.7, 17.8, 12.7, and 14 Myr, in order of increasing plotted $Z$. Each upper limit is derived by scaling the corresponding lower limit to a runaway time of 10 Myr (our assumed lifetime for a gas-rich disk) using the empirical relation $t_{\rm run} \propto M_{\rm core}^{-3.93}$ (Paper I). Analytic predictions for $M_{\rm crit,core}$ (Paper II) are overplotted as curves. The dashed curve is computed using gas-to-core mass ratio GCR = 0.5, time $t = 10$ Myr, the dimensionless adiabatic gradient $\nabla_{\rm ad} = 0.17$, and the radiative-convective boundary temperature $T_{\rm rcb} = 2500$ K. The dashed–dotted curve is the same except that it uses $T_{\rm rcb}$ as computed from the numerical model for every black datum.

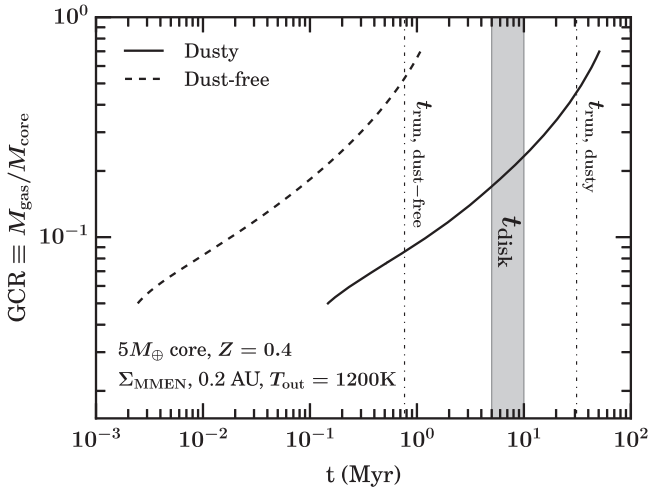


**Figure 2.** A tale of two opacities: evolution of gas-to-core mass ratios for a 5 $M_\oplus$ core situated at 0.2 AU in a metal-enhanced ($Z = 0.4$) MMEN with either "dusty" or "dust-free" opacities. "Dusty" opacities assume a grain size distribution similar to that of the interstellar medium (Ferguson et al. 2005); "dust-free" opacities eliminate the contribution from grains, simulating their removal by coagulation and settling (e.g., Ormel 2014). For Figures 2 and 3, the nebular temperature $T_{\rm out}$ was enhanced by a factor of 1.6 above the MMEN value to 1200 K; this enhancement (which is still physically plausible; see, e.g., D'Alessio et al. 2001) was necessary to numerically resolve the outer radiative zone. Runaway times mark when model cooling luminosities reach their minima (see Papers I and II) and are indicated by vertical dotted–dashed lines. Dust-free atmospheres run away well before the disk dissipation time $t_{\rm disk} \sim 5$–$10$ Myr.

### 2.2. Dust Coagulation: Low-κ Catastrophe

Opacity gains by dust depend on the grain size distribution and the degree to which dust is well mixed in gas. Dust coagulation can wipe out these gains, not only by reducing the surface area of dust per unit mass (e.g., Piso et al. 2015), but also by speeding the gravitational sedimentation of dust out of the atmosphere's radiative layers (Mordasini et al. 2014; Ormel 2014).

Grain growth in disks can be fast, especially at the high densities that prevail inside 1 AU (e.g., Blum & Wurm 2000; Windmark et al. 2012). Grains need only grow to sizes $\gtrsim 0.1$ mm for the gas opacity to overwhelm the dust opacity (in the Rosseland mean sense). Dust can also be removed by drifting to deeper, hotter layers where they sublimate. This last concern applies to atmospheres that are purely radiative (assumed static) from the outermost surface layers down to the sublimation front. For our models at ∼0.1 AU, such conditions obtain for GCRs $> 0.1$. We estimate settling times in such radiative layers to be ∼1 Myr—shorter than disk lifetimes of ∼5–10 Myr—for $\mu$m-sized grains. Larger grains settle even faster.

We demonstrate in Figure 2 the drastic effect of rapid dust coagulation and sedimentation: even at $Z = 0.4$, $5M_\oplus$ cores with no dust in their atmospheres run away within the disk lifetime.

Dust-free atmospheres accrete faster than dusty atmospheres because removing the opacity from dust lifts the rcb to higher altitudes where atmospheres cool faster (Paper II). The reason for the higher altitude of the rcb is as follows. In dusty atmospheres, a radiative window is necessarily opened in the planet's deep interior where temperatures are high enough ($T \gtrsim$ 2000 K) for dust to sublimate, dropping the opacity $\kappa$ by 2 orders of magnitude and facilitating energy transport by radiation. This radiative window closes at the $H_2$ sublimation front at $T \sim 2500$ K; here lies the innermost rcb, where $\kappa$ surges back up from the creation of $H^-$ ions. Dust-free atmospheres have no such radiative window because there is no dust to sublimate. Their rcb's are located near their outermost boundaries, at the base of a nearly isothermal radiative layer that connects directly to the ambient disk. Figure 3 reveals the rcb in a dust-free atmosphere to occur at $T \sim 1500$ K, close to the nebular temperature $T_{\rm out} = 1200$ K. The dust-free rcb is located at a higher altitude—where density $\rho$ and opacity $\kappa$ are lower—as compared to the innermost rcb in a dusty atmosphere. Because an envelope's cooling luminosity is controlled at its rcb where $L \propto 1/(\rho\kappa)$ (e.g., Equation (33) in Paper I), the lower $\rho$ and $\kappa$ characterizing the rcb in a dust-free atmosphere leads to larger $L$, faster cooling, and more rapid accretion of gas (see also Paper II).

## 3. ACQUIRING ATMOSPHERES IN GAS-POOR NEBULAE (SCENARIO B)

A way out of the high-$\mu$ and low-$\kappa$ catastrophes (Sections 2.1–2.2) is to form super-Earths in nebulae depleted in gas. Less ambient gas would obviously seem to reduce the likelihood of runaway. It does, but final GCRs are remarkably insensitive to ambient nebular densities, as we will stress later in this section. Just as important, if not more so, is the limited time available for gas accretion in scenario (b): staging envelope accretion during the era of disk dispersal sets a stricter time limit on how much gas a core can accrete. Observations of transitional protoplanetary disks suggest that their inner regions clear in $\lesssim$10% of the disk's total lifetime (Alexander et al. 2014). If close-in cores start accreting gas

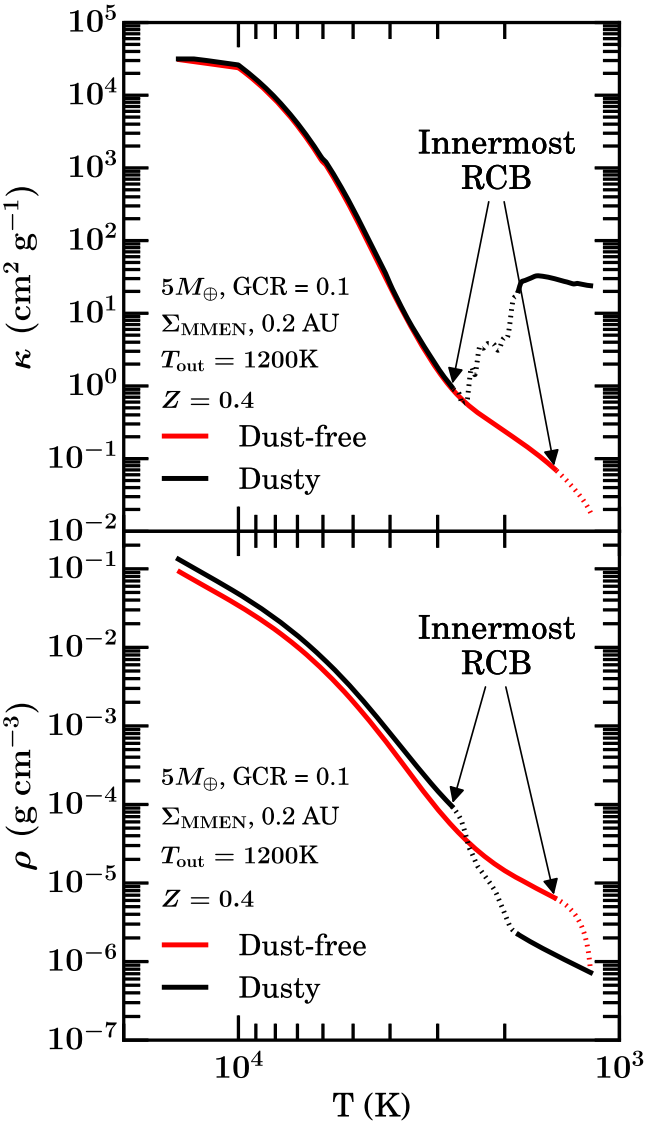


**Figure 3.** The effect of dust on the radiative-convective boundary (rcb). Top and bottom panels show opacity and density profiles of the $5M_\oplus$ models presented in Figure 2 (nebular temperature enhanced by a factor of 1.6 at 0.2 AU to 1200 K), evaluated at GCR = 0.1, for dusty vs. dust-free opacities (the latter is our proxy for grain growth and sedimentation). Dashed lines delineate radiative zones while solid lines trace convective zones. Dust sublimation in a dusty atmosphere forces $\kappa$ to drop by approximately 2 orders of magnitude, opens a radiative window between 2000 and 2700 K, and pushes the innermost rcb (the one that controls the overall luminosity of the atmosphere) to greater depth. By comparison, the rcb in a dust-free atmosphere is situated at a higher altitude where $\kappa$, $\rho$, and $T$ are lower by factors of 14, 14, and 2, respectively; the upshot is that $L \propto T^3/\rho\kappa$ increases by a factor of 30. The higher $L$ explains the shorter $t_{\rm run,dust\text{-}free}$ in Figure 2.

during this final clearing phase, then they have $\lesssim$1 Myr to build their atmospheres rather than ∼10 Myr; they run out of time before running away.

In addition to the advantages presented by depleted, short-lived nebulae in avoiding gas giant formation, there is actually a physical reason to believe super-Earth cores of mass ∼2–20$M_\oplus$ form in gas-poor environments. Cores assemble from the mergers of smaller "protocores," whose eccentricities need to grow large enough for their orbits to cross. Mutual gravitational scatterings between protocores can excite eccentricities, but must compete against eccentricity damping by tidal torques (a.k.a. dynamical friction) exerted by gas. Core formation is therefore delayed until the gas disk depletes sufficiently that eccentricity damping no longer prevents mergers.[6]

In Section 3.1, we estimate the extent to which nebular gas densities can be reduced and still give rise to the GCRs inferred for super-Earths. There we also connect our idea that super-Earths form in gas-poor disks to theories of transitional disks and disk dispersal. Whether the gas depletion factors we require are compatible with protocore mergers and core assembly is examined in Section 3.2.

### 3.1. Gas Depletion Factors Compatible with GCRs and Disk Dispersal Theories

One might think that for a planet to achieve a GCR $\gtrsim$ 1%, it needs to form in a disk whose gas-to-solid ratio $\gtrsim$ 1%. Such reasoning is too restrictive; the argument presumes that once a rocky core consumes all the gas in its immediate vicinity, it cannot accrete more because its local gas reservoir is not replenished. But replenishment is the hallmark of accretion disks: the inner disk, where cores reside, can be resupplied with fresh gas by diffusion from the outer disk. In principle, a close-in core can sit in an environment nearly devoid of gas, yet still acquire an atmospheric mass fraction $\gtrsim$1%, provided gas is fed to it from the outside for a long enough time (i.e., over the ∼Myr timescales that our calculations cover; the assumption of all our models is that gas densities at the planet's outer boundary—the Hill or Bondi radius—are fixed in time).

Figure 4 shows how this principle is put into practice, underscoring just how little ambient disk gas is needed to reproduce observed GCRs. A $5M_\oplus$ core can reside in a disk whose gas density is depleted relative to the MMEN by a factor as large as $10^7$ and still emerge with a GCR of ∼2% at the end of 1 Myr. The rate at which a core accretes gas hardly depends on the local nebular density; the rate of accretion is controlled by the rate of cooling, and cooling is regulated at rcb's, which for the dusty atmospheres featured in Figure 4 are isolated from the external nebula. All other factors being equal, the final GCR changes by a mere factor of 2 as the nebular depletion factor runs from $10^2$ to $10^7$ (Figure 4, right panel). This insensitivity of the final GCR to nebular density applies only to disks that are depleted by at least factors of ∼10 relative to the MMEN; in the left panel of Figure 4, we observe a larger-than-expected increase in the final GCR between the full $\Sigma_{\rm MMEN}$ case and more depleted cases. One reason for this jump is the longer lifetime of a gas-rich disk (10 Myr) versus that of a depleted disk (1 Myr). Another reason is that for the gas-rich case, the outermost layers of dusty atmospheres are convective, whereas for most of the gas-poor cases, they are radiative. Because radiative layers have steep density gradients, they more strongly decouple the rcb from the nebula at large.

Depleted inner disks of the kind envisioned here bring to mind transitional protoplanetary disks having central cavities or "holes" (for a review, see Espaillat et al. 2014). A crucial element of our picture is that what little gas pervades the inner disk (where super-Earths live) is continuously replenished by gas from the outer disk, over timescales not much shorter than ∼1 Myr. It is both encouraging and surprising that real-life transitional disks qualitatively fit this picture: they have holes

[6] This argument is subject to the possibility that gas might actually excite eccentricities, either resonantly by Lindblad torques (Goldreich & Sari 2003; Duffell & Chiang 2015) or stochastically by turbulent density fluctuations (e.g., Ogihara et al. 2007, and references therein).

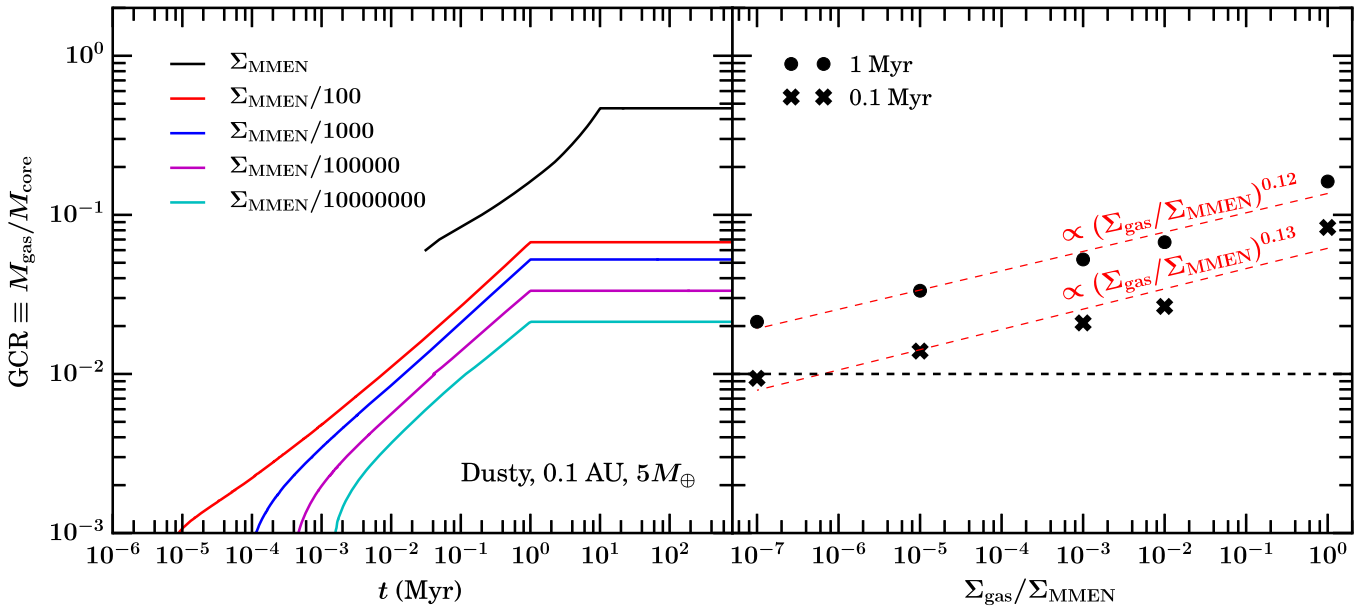


**Figure 4.** Under scenario (b), there is an impressive variety of short-lived, gas-poor nebulae that can generate GCRs on the order of a few percent, similar to values inferred for super-Earths. Gas surface densities can be depleted by more than five orders of magnitude relative to the MMEN, and GCRs for $5M_\oplus$ cores at the end of 0.1 Myr will still remain above 0.01 (right panel, crosses). If atmospheric growth is allowed to proceed for 1 Myr (circles), then the nebula can be depleted by more than eight orders of magnitude and GCRs can stay above 0.01 (assuming the fitted red dashed line can be extrapolated). Colored curves in the left panel denote various depleted nebulae whose lifetimes are capped at $t = 1$ Myr; these curves show that final GCRs $\geqslant 0.01$ can be attained as long as the disk persists for $\gtrsim 8$ kyr, which is reassuringly much shorter than typically modeled disk clearing timescales. The black curve is a sample evolution from the disfavored scenario (a); here the planet barely escapes runaway in an undepleted disk lasting $t = 10$ Myr. All models with nebular surface density $\Sigma_{\rm gas} < \Sigma_{\rm MMEN}/10^5$ are calculated with opacities extrapolated to low density (see footnote 7).

yet deliver gas onto their central stars at rates comparable to those of disks without holes. To resolve the paradox of simultaneous transparency and accretion, Rosenfeld et al. (2014) posited that gas radial velocities are much larger inside the hole than outside the hole, as gas surface density $\Sigma_{\rm gas}$ varies inversely with inflow velocity at fixed disk accretion rate. They entertained the possibility that gas radial velocities could approach Keplerian velocities; found observational evidence for free-fall velocities in the transitional disk HD 142527; and speculated that gravitational torques by massive companions could drive these large velocities (see also Casassus et al. 2015). We term this idea "dynamic accretion," as distinct from the traditional and slower "viscous accretion." Technically the optically thin cavities of transitional disks conflict with our model for nebular accretion of atmospheres, which assumes the disk to be optically thick. We defer consideration of how core accretion works in optically thin disks to a future study.

In the left panel of Figure 5, we indicate with a colored bar the nebular gas densities that can generate $0.01 \leqslant$ GCR $\leqslant 0.1$ within 1 Myr for $5M_\oplus$ cores having dusty atmospheres at 0.1 AU. The range of gas depletion factors $\Sigma_{\rm gas}/\Sigma_{\rm MMEN}$ is enormous, spanning nine orders of magnitude.[7] There is complementary flexibility in the accretion time, which need not be 1 Myr; e.g., Figure 4 shows that a mere 8 kyr is required to attain GCR $= 0.01$ if $\Sigma_{\rm gas} = \Sigma_{\rm MMEN}/100$. Thus there is no need to fine-tune either disk properties or the accretion time in scenario (b); this conclusion will be supported further by calculations below.

Whatever drives dynamic accretion (e.g., a massive perturber, or disk self-gravity) may actually de-stabilize the orbits of super-Earths. An alternate, less dramatic way to generate inner disk holes containing accreting gas is through "photoevaporation-starved accretion" (Clarke et al. 2001; Drake et al. 2009; Owen et al. 2011, 2012; Alexander et al. 2014). In this scenario, the disk interior to ~1 AU becomes starved when the disk outside ~1 AU is blown out by a photoevaporative wind before it can diffuse in. A gap is formed near ~1 AU, and the starved interior disk has no choice but to viscously drain onto the star and be severely depleted. Super-Earth cores at ~0.1 AU are fed by gas that viscously diffuses from ~1 AU, but only for as long as it takes gas to diffuse from that distance. This diffusion time is short, on the order of ~0.1 Myr (see, e.g., Figure 9 of Owen et al. 2011). A time limit of 0.1 Myr for nebular accretion of planetary atmospheres restricts the range of allowed gas depletion factors to those shown in the colored bar of the right panel of Figure 5. The range of disk conditions compatible with GCR $\geqslant 0.01$ is narrower for an accretion time of 0.1 Myr versus 1 Myr (compare right versus left panels). But the range of allowed disk gas densities in the more time-limited case—covering more than six orders of magnitude—still impresses. Again, there is no indication of a fine-tuning problem.

Figure 6 is the same as Figure 5, except that the colored bars are computed for dust-free rather than dusty atmospheres. Dust-free envelopes cool and accrete faster than dusty envelopes and therefore require more severe depletion of the ambient gas disk to reach a given GCR at a given time. Nevertheless, dust-free envelopes exhibit the same robustness and tell the same story

[7] Nebulae that are depleted by more than five orders of magnitude with respect to the MMEN fall off the opacity table by Ferguson et al. (2005) for dusty envelopes. For these low-density nebulae, we extrapolate the opacity table by fitting a power law $\kappa \propto \rho^\alpha T^\beta$ for $-11 \leqslant \log \rho(\,{\rm g\,cm^{-3}}) \leqslant -9$ and $2.7 \leqslant \log T\,({\rm K}) \leqslant 3$.

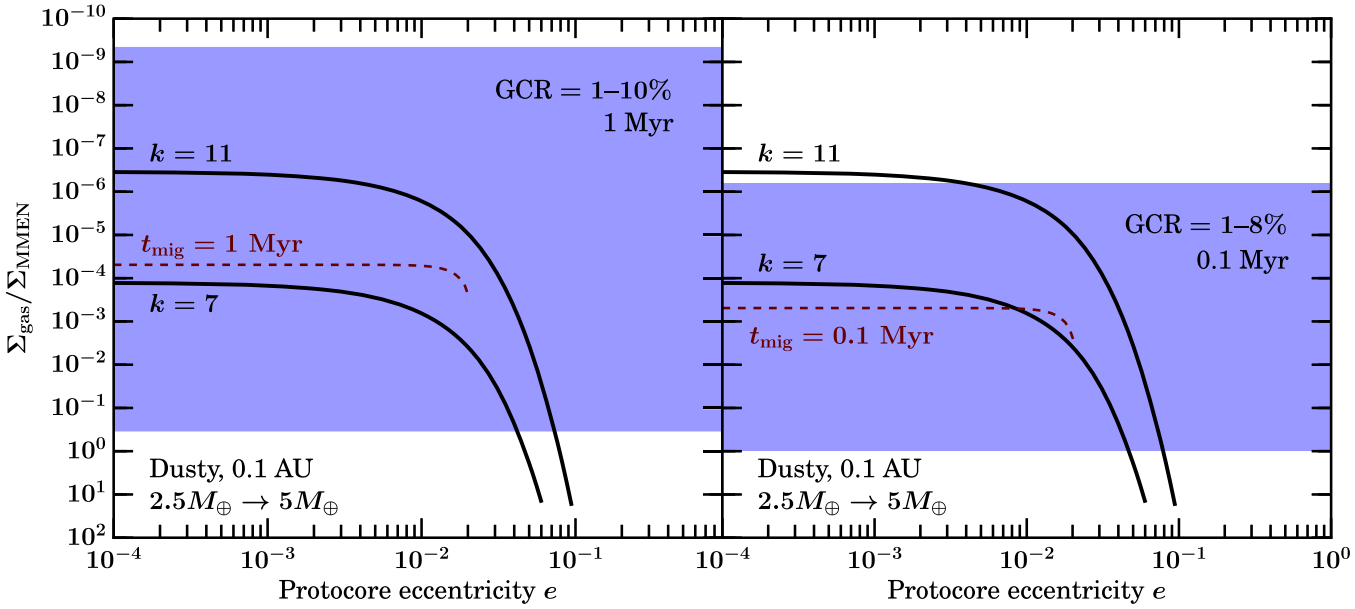


**Figure 5.** Super-Earth formation in a gas-poor nebula (scenario b) accommodates a wide variety of disk environments and can preserve planets against orbital migration. Solid curves trace the amount of disk gas depletion required for an ensemble of $2.5M_\oplus$ protocores to "viscously stir" one another onto crossing orbits against gas dynamical friction, thereby merging into $5M_\oplus$ cores. Each curve is calculated from the condition $t_{\rm damp} = 0.1t_X$ evaluated at $a = 0.1$ AU, and terminates at max $e = kR_{\rm mH}/2a$, the orbit-crossing value. Orbital spacings $k$ (in units of mutual Hill radii $R_{\rm mH}$) of 7 and 11 bracket possible protocore spacings as estimated from *Kepler* data (see text). Blue bars denote the gas depletion factors for which a $5M_\oplus$ core at 0.1 AU can accrete a dusty atmosphere having GCR = 0.01–0.1 within 1 Myr (left panel) and 0.1 Myr (right panel); the time limit of 0.1 Myr is inspired by the "photoevaporation-starved" models of Owen et al. (2011) in which the disk inside ∼1 AU drains away on that $e$-folding time. Note that within 0.1 Myr, $5M_\oplus$ cores accrete up to only 8% GCR in a full MMEN (right panel). That the blue bars overlap the $k$-curves means that the constraints imposed by planetary GCRs and by protocore mergers can be simultaneously satisfied; indeed there are orders of magnitude of play in the blue bars, reflecting the insensitivity of atmospheric growth rates to the ambient nebular density (see also Figure 4). Red dashed lines mark the gas surface densities for which the Type I migration timescale $t_{\rm mig}$ (Equation (31) of Papaloizou & Larwood 2000) equals the assumed gas disk lifetime, evaluated for a $5M_\oplus$ core at 0.1 AU. For the most part, the constraints from protocore mergers ($k$-curves) sit safely above the migration constraint, indicating that migration may be negligible for most super-Earth systems.

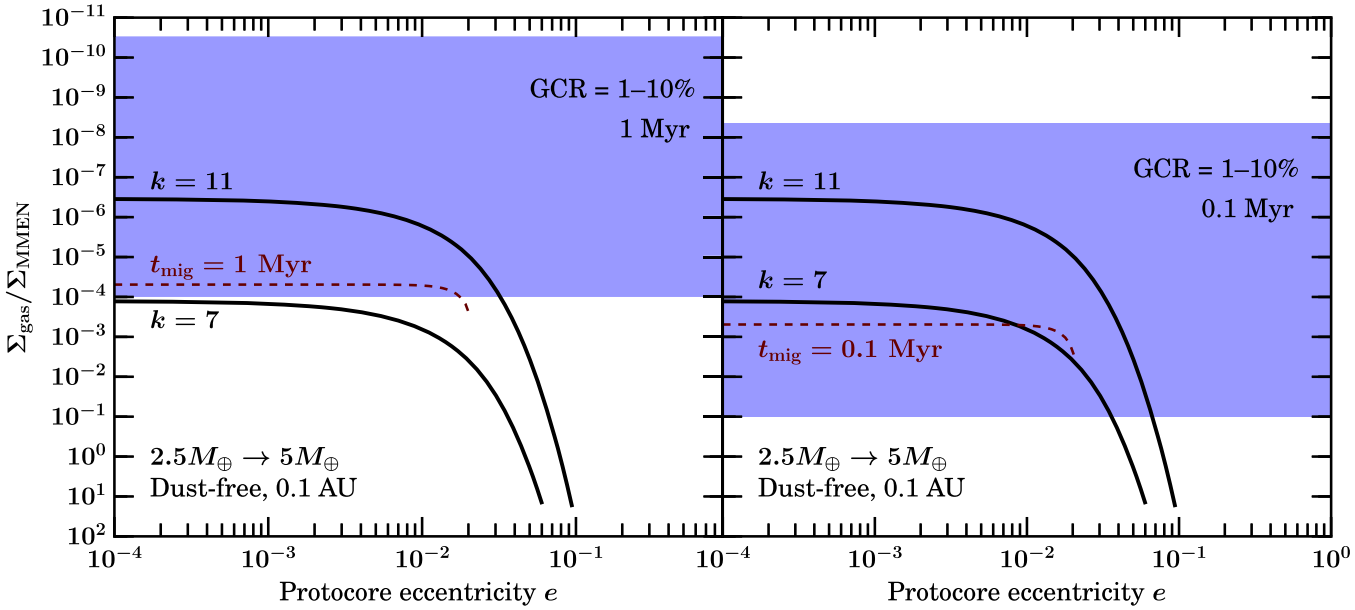


**Figure 6.** Same as Figure 5 but for dust-free envelopes. The lower limits of colored bars correspond to nebular surface densities $\Sigma_{\rm gas}$ for which $5M_\oplus$ cores can emerge with GCR = 10% within 1 Myr (left panel) and 0.1 Myr (right panel). The upper limits of colored bars correspond to gas depletion factors consistent with GCR = 1%, and are determined by extrapolating a power-law fit to GCR vs. $\Sigma_{\rm gas}$ (such extrapolation is necessary since neither our tabulated dust-free opacities nor analytic fits to those opacities extend to the lowest densities relevant here). Gas depletion factors consistent with super-Earth GCRs span about 7–8 orders of magnitude, reflecting (as was the case for the dusty envelopes of Figure 5) the insensitivity of the cooling rates of envelopes to ambient gas densities.

as their dusty counterparts: surface densities $\Sigma_{\rm gas}$ can range across 7–8 orders of magnitude, and super-Earth cores can coagulate at ∼0.1 AU and accrete dust-free atmospheres having GCR ∼1%–10% within 0.1–1 Myr.

In Section 3.2 below, we compare the gas depletion factors computed here to those needed to coagulate rocky cores against gas dynamical friction. We also assess whether super-Earth cores migrate in depleted gas disks (preview: they do not).

### 3.2. Gas Depletion Factors Required to Merge Protocores

Unless 2–20$M_\oplus$ cores are born as isolation masses from disks with high solid surface density (e.g., Dawson et al. 2015b), they form instead from collisions of smaller protocores (a.k.a. oligarchs). Whether the target values of $\Sigma_{\rm gas}/\Sigma_{\rm MMEN}$ estimated in Section 3.1 are low enough to promote orbital instability and mergers of protocores depends on protocore orbital spacings and eccentricities (and inclinations; Dawson et al. 2015b). Mergers widen orbital separations, significantly increasing orbit-crossing timescales for subsequent mergers (e.g., Chambers et al. 1996, Zhou et al. 2007). Consequently, the time it takes a set of isolation masses to merge into a system of super-Earth cores is largely determined by the final doubling: the transformation of 1–10 $M_\oplus$ protocores into 2–20 $M_\oplus$ cores.

We determine how depleted ambient gas disks must be to effect the final doubling of protocores into full-fledged super-Earth cores. Formally, we solve for the conditions under which the eccentricity damping timescale $t_{\rm damp}$ exceeds ~0.1 of the orbit crossing timescale $t_X$ (the factor of 0.1 is empirically determined by Iwasaki et al. 2001; see also Kominami & Ida 2002).[8] Zhou et al. (2007) give the following empirical fitting formulae for $t_X$ for an ensemble of nine equal-mass protocores situated at a mean semimajor axis $a$, with adjacent pairs separated by $\Delta a$:

$$
\begin{aligned}
h &= \frac{k}{2}\left(\frac{2M}{3M_*}\right)^{1/3} \\
k &= \Delta a/R_{\rm mH} \\
R_{\rm mH} &= \left(\frac{2M}{3M_*}\right)^{1/3} a \\
A &= -2 + e/h - 0.27\log_{10}\left(\frac{M}{M_*}\right) \\
B &= 18.7 - 16.8e/h + (1.1 - 1.2e/h)\log_{10}\left(\frac{M}{M_*}\right) \\
t_X &= 10^{A+B\log_{10}(k/2.3)}\ \text{years}\left(\frac{a}{\rm AU}\right)^{1.5}
\end{aligned}
\tag{1}
$$

where $k$ is the orbital spacing in mutual Hill radii $R_{\rm mH}$, $e$ is the eccentricity of a protocore, $M$ is the mass of a protocore, and $M_*$ is the mass of the host star. Zhou et al. (2007) provide results only for protocores situated near $a = 1$ AU; we have added a factor of $(a/{\rm AU})^{1.5}$ to Equation (1) so that we can scale down to shorter orbital periods at $a \sim 0.1$ AU where many *Kepler* planets reside. The true scaling factor has not been carefully measured and may differ slightly. Our calculations below set $a = 0.1$ AU but clearly other formation distances are possible.

Eccentricity damping timescales are typically quoted for planets with small eccentricities $e \ll c_{\rm s}/v_{\rm K}$, where $c_{\rm s}$ is the gas sound speed and $v_{\rm K}$ is the Keplerian velocity. Papaloizou & Larwood (2000) find that when $e > c_{\rm s}/v_{\rm K}$, damping becomes less efficient and reduces to the form of classical dynamical friction ($\dot{e} \propto -1/e^2$). We modify the eccentricity damping timescale of Kominami & Ida (2002) to account for high eccentricity as follows:

$$
t_{\rm damp} = \frac{e}{|\dot{e}|} = 0.5\ \text{years}\left(\frac{T}{1000\ \rm K}\right)^{1.5}\left(\frac{6\times10^{-6}\ \rm g\ cm^{-3}}{\rho}\right)\left(\frac{M_\oplus}{M}\right)\left[1+\frac{1}{4}\left(\frac{e}{c_{\rm s}/v_{\rm K}}\right)^3\right] \tag{2}
$$

where $T$ is the gas temperature, $\rho$ is the gas density, and the factor in square brackets that depends on $e$ is taken from Equation (32) of Papaloizou & Larwood (2000). The volumetric density $\rho$ relates to the surface density via $\Sigma_{\rm gas} = \sqrt{2\pi}\rho c_{\rm s} a/v_{\rm K}$.

Values of $\Sigma_{\rm gas}/\Sigma_{\rm MMEN}$ implied by the condition $t_{\rm damp} > 0.1 \times t_X$ are shown as solid curves in Figure 5. Our plotted $k$-values of 7 and 11 were chosen as follows. Observed *Kepler* multi-planet systems (with multiplicity $\geqslant 5$) have a present-day mean orbital spacing of $k \simeq 14 \pm 3.4$ (taken from the "intrinsic" $k$ distribution of Pu & Wu 2015; see their Figure 7). Combining this range with the assumption that protocores maintain uniform masses and spacings as they merge, we estimate that just prior to the last doubling, $k \sim (10.6\text{–}17.4) \times 2^{-2/3} \sim 6.7\text{–}11$ (the absolute spacing decreases by a factor of 2, and protocores are half as massive as final cores so $R_{\rm mH}$ decreases by $2^{1/3}$).

The smaller the protocore eccentricities $e$, the smaller $\Sigma_{\rm gas}$ must be to effect mergers. The target gas depletion factors derived in Section 3.1 from GCR considerations are overlaid as colored bars in Figure 5. For the most part, the $k$-curves intersect the colored bars. In other words, the constraints imposed by super-Earth atmospheric mass fractions (colored bars) and by super-Earth core formation ($k$-curves) can be simultaneously satisfied for a wide range of protocore orbital spacings and eccentricities, and a huge variety of gas-poor inner disks (fed by gas-rich outer disks), all over timescales of 0.1–1 Myr.

More precise determinations of the gas depletion factors and the orbital properties of protocores required for core assembly —i.e., better $k$-curves—can be obtained from $N$-body simulations that include gas damping and that are tailored for close-in super-Earths. Kominami & Ida (2002) and Ogihara et al. (2007) carried out similar calculations, but for parameters specific to solar system terrestrial planets.

We close this section by noting that we expect eccentricities of fully coagulated super-Earth cores to be damped to varying degrees by residual gas (see, e.g., Agnor & Ward 2002). Just after their last doubling, cores should have eccentricities of order $e \sim 1/2 \times kR_{\rm mH}/2a \sim 0.03\text{–}0.05$ (the final $e$ should be the orbit-crossing value just prior to the last doubling—these are the values at which the $k$-curves in Figure 5 terminate—multiplied by 1/2 to account for momentum conservation in inelastic collisions). These eccentricities can be damped by whatever gas remains: we insert into Equation (2) these $e$'s, together with the depleted densities indicated by the $k$-curves in Figure 5 ($\rho/\rho_{\rm MMEN} \sim 10^{-4}$ for $k = 7$, and $4 \times 10^{-7}$ for $k = 11$). For $k = 7$, we find that 5 $M_\oplus$ cores at 0.1 AU starting with $e \sim 0.03$ have an eccentricity damping timescale $t_{\rm damp} \sim 0.002$ Myr; this is much shorter than either the orbit crossing time $t_X \sim 0.2$ Myr or the depletion time of a gas-poor disk $t_{\rm disk} \sim 0.1\text{–}1$ Myr, indicating that super-Earths created under these conditions should have their orbits circularized. For

[8] For this last doubling, protocores are so widely spaced (the number of Hill-radius spacings $k > 5$) that the particle-in-a-box approximation (e.g., Safronov 1972, Goldreich et al. 2004) likely fails (Ford & Chiang 2007).

$k = 11$, $t_{\rm damp} \sim 1$ Myr and $t_X \sim 27$ Myr. Because $t_{\rm damp}$ is now comparable to the upper limit of $t_{\rm disk}$, super-Earths created under these conditions may have their starting eccentricities of ~0.05 decreased by at most a factor of order unity. Putting the results of $k = 7$ and $k = 11$ together, we argue that super-Earth eccentricities today should range anywhere from 0 to 0.05. These crude considerations align with observations: for *Kepler* multiplanet systems around host stars amenable to asteroseismic density measurements, Van Eylen & Albrecht (2015) measure rms eccentricities of ~0.049 from the distribution of transit durations; Xie et al. (2015, submitted) arrive at similar results with a significantly larger sample of planets using *LAMOST*.[9]

## 4. SUPER-PUFFS AS MIGRATED DUST-FREE WORLDS

*Kepler* has discovered a relatively rare population of especially large ($R \gtrsim 4R_\oplus$) and low mass ($M \lesssim 6M_\oplus$) planets. We refer to them as "super-puffs." Super-puffs are the exception, not the rule: planets with $R > 4R_\oplus$ are more than an order-of-magnitude more rare at orbital periods < 50 days than planets with $R < 4R_\oplus$ (Fressin et al. 2013).[10] Examples include Kepler-51b (Steffen et al. 2013), a $2.1^{+1.5}_{-0.8}\,M_\oplus$ planet of size $7.1 \pm 0.3$ $R_\oplus$ orbiting its host star at 0.2 AU (Masuda 2014). Another example is Kepler-79 d (Steffen et al. 2010), a $6.0^{+2.1}_{-1.6}\,M_\oplus$ planet of size $7.16^{+0.13}_{-0.16}\,R_\oplus$ orbiting its host star at 0.3 AU (Jontof-Hutter et al. 2014). The inferred GCRs of these two planets are 7%–28% and 33%–40%, respectively (Lopez & Fortney 2014).

Can we fit a few super-puffs into our theory of in situ gas accretion from depleted nebulae? Our numerical model gives GCR ~ 1% for a $2\,M_\oplus$ core (dusty atmosphere; 0.1 AU; depleted $\Sigma_{\rm MMEN}/200$ nebula lasting $t = 1$ Myr). Unfortunately, this GCR is much too low compared to that of Kepler-51b. Others have noted similar difficulties with $R \gtrsim 4$ $R_\oplus$ and $M \lesssim 5M_\oplus$ planets accreting enough nebular gas in situ at ~0.1 AU (Ikoma & Hori 2012; Inamdar & Schlichting 2015).

Nebular accretion can still explain super-puffs (what other option is there?)—perhaps not at ~0.1 AU where they are currently found, but rather at distances beyond ~1 AU—and with the additional proviso that atmospheres be dust-free. At larger orbital distances, dust-free envelopes cool and accrete faster than do dusty envelopes, not just because of their reduced opacity (Figure 2; see also Piso et al. 2015), but also because dust-free atmospheres are responsive to the colder temperatures and lower densities characterizing the outer disk.[11] The rcb's of dust-free atmospheres have temperatures approximately equal to the ambient disk temperature. Because disk temperature decreases with increasing orbital distance, and because dust-free opacities diminish with decreasing temperature, dust-free atmospheres become optically thinner farther away from the host star. It follows that more distant, cooler, dust-free planets cool more easily and grow faster (Paper II).

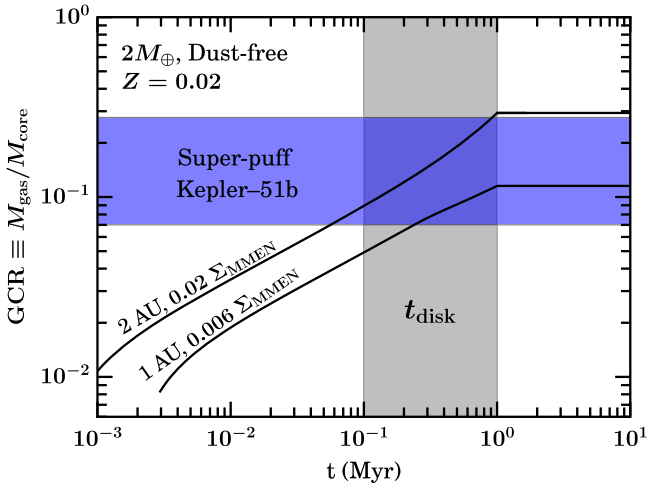


**Figure 7.** Birth of a dust-free super-puff at 1–2 AU. The blue region delineates the range of possible envelope fractions for $2M_\oplus$ super-puff Kepler-51b, as calculated by Lopez & Fortney (2014), and the vertical gray bar denotes the timescales—0.1–1 Myr—over which the gas-poor disk finally clears. (the clearing timescale $t_{\rm disk}$ for a gas-poor disk is $\lesssim 10\%$ that of a gas-rich disk). Solid curves correspond to $2M_\oplus$ cores embedded in nebulae whose surface densities (annotated on the plot) are chosen to give a Type I migration timescale $a/\dot{a} = 1$ Myr. The relatively large GCRs characterizing super-puffs can be achieved by having cores with dust-free atmospheres form at larger orbital distances where nebular gas is cooler and less opaque.

Appealing to nebular accretion beyond ~1 AU requires that we invoke orbital migration to transport super-puffs to their current observed locations at ~0.1 AU. Convergent migration of multiple planets can lead to capture into mean-motion resonances. In this regard we find it intriguing that all three members of the Kepler-51 system (2 confirmed + 1 candidate; all are puffy, having $R > 4R_\oplus$) are situated near a 1:2:3 resonance (Masuda 2014). The Kepler-79 system (3 super-Earths + 1 super-puff) may also be linked by a 1:2:4:6 resonant chain (Jontof-Hutter et al. 2014).

Type I migration requires gas. Timing super-puff migration with disk dispersal—in particular, the severe dispersal required to form super-Earths (Section 3)—may be tricky. It helps that super-puff cores have less mass than super-Earth cores and can therefore coagulate more readily in the face of gas dynamical friction (cf. Section 3.2). The right sequence of events might play out as follows: super-puff cores coagulate—perhaps as isolation masses—and accrete their gas envelopes in a relatively gas-rich disk outside 1 AU; they migrate inward, possibly at the same time as they are amassing atmospheres; they get caught into resonance with interior planets (either super-puffs or super-Earths); and are finally parked inside 1 AU as the gas disk—now in its transitional phase—clears from the inside out (i.e., as the central gas cavity grows from small radius to large radius; cf. Chiang & Murray-Clay 2007; Alexander et al. 2014). The rarity of close-in super-puffs might

[9] Other constraints on eccentricities come from statistical analyses of super-Earth transit-timing variations (TTVs). These constraints—namely, rms eccentricities of 0.018 (Hadden & Lithwick 2014)—are relevant for systems near mean-motion resonance; as such they may not be relevant for run-of-the-mill super-Earths which are not resonant.

[10] Super-puffs are a subset of what some call "sub-Saturns."

[11] Atmospheres can also be enriched with water beyond the nebular ice line. Water-rich atmospheres not only have high mean molecular weight, but can also have their density gradients steepened by the thermostating effects of sublimating ice (Hori & Ikoma 2011; Venturini et al. 2015). More isothermal and higher $\mu$ atmospheres are more susceptible to gravitational collapse onto low-mass cores on Myr timescales; Stevenson (1984) theorized that sub-Earth-mass cores could rapidly nucleate gas giants in icy nebulae, dubbing such planets "superganymedean puffballs." The amount of water enrichment required to significantly accelerate gas accretion is large: $Z \gtrsim 0.6$ (e.g., Figure 1 of Venturini et al. 2015). But too large a $Z$ would render these planets "water worlds" or "steam worlds," with radii too small to match those of super-puffs (e.g., Figure 7 of Lopez & Fortney 2014). Because $Z$ would need to be fine-tuned to avoid water worlds but still produce super-puffs, we disfavor the idea that super-puffs accreted their thick envelopes by virtue of their water content; at the same time, we do expect super-puffs to have more water than closer-in super-Earths.

reflect the difficulty in orchestrating this sequence with favorable disk parameters.

Uncertainties in migration history notwithstanding, Figure 7 demonstrates that super-puffs can readily acquire their thick envelopes at large distances $\gtrsim$1 AU. Placed in a disk whose gas density is large enough to permit inward migration over ∼1 Myr, a $2M_\oplus$ core at 1–2 AU can accrete a dust-free atmosphere with GCR ∼10%–30%, successfully reproducing the properties of Kepler-51b.

## 5. SUMMARY AND OUTLOOK

*Kepler* super-Earths have core masses large enough to nucleate gas giants, yet have atmospheres that are modest by mass (e.g., Lopez & Fortney 2014; Wolfgang & Lopez 2015). In Paper I, we proposed two possible scenarios for making super-Earths over Jupiters: either (a) they form in gas-rich nebulae sufficiently enriched in dust that atmospheres cool and therefore accrete only slowly; or (b) they form in gas-poor (but not gas-empty) disks, with no constraint on dust content. Having gained additional insights into the physics of nebular accretion from Paper II, we have in the present work re-evaluated these two scenarios to determine which is more plausible.

Although strong radial gradients in dust content are expected in protoplanetary disks (see, e.g., Paper I), no amount of dust can save super-Earth atmospheres from going runaway. Dust does not just increase the opacity $\kappa$; it also increases (when sublimated at atmospheric depth) the mean molecular weight $\mu$, and high-$\mu$ atmospheres are prone to gravitational collapse. At metallicities $Z \gtrsim 0.2$, the deadly side effects of higher $\mu$ overwhelm the benefits of higher $\kappa$. No cure is available for $\sim 10M_\oplus$ cores in gas-rich nebulae lasting ∼10 Myr; they are fated to spawn gas giants.

This leaves us with the gas-poor environment of scenario (b). Gas-poor conditions prevail just before the disk disappears completely; such conditions are short-lived (∼0.1–1 Myr versus ∼10 Myr) which helps to stave off runaway (see Figure 5). A depleted nebula is also motivated on independent grounds by the need for gas to deplete before cores can coagulate. As disk gas vacates (either by viscously draining onto the star or by being blown off in a wind), dynamical friction weakens to the point where protocores can gravitationally stir each other onto crossing orbits and merge to become super-Earths. The degree of gas depletion required to enable protocores to merge can be severe: gas surface densities of disks may need to be $10^4$–$10^7$ times lower than those of a conventional, solar-composition minimum-mass nebula for viscous stirring to overcome gas dynamical friction. Such tiny amounts of gas might be thought to be insufficient to furnish planetary atmospheric mass fractions >1%. This is fortunately not at all the case—gas accretion rates onto planets are incredibly insensitive to ambient disk gas densities (see also Paper II). This feature of nebular accretion should dispel concerns that disk conditions need to be fine-tuned to form super-Earth atmospheres. As long as some gas can be siphoned from the outer disk to feed the inner disk for 0.1–1 Myr, rocky cores in the inner disk can successfully pick up envelopes of the required mass. The picture we are led to—super-Earths forming in an inner disk that contains only wisps of gas leaked from a gas-rich outer disk—is reminiscent of transitional protoplanetary disks, whose central cavities are not entirely void but contain inflowing gas. So little gas is tolerated during the era of core assembly that super-Earths are safe from wholesale orbital migration driven by gas disk torques: super-Earths may have formed in situ.

Nebular accretion under scenario (b) can also accommodate super-puffs—a rare class of large radius ($R \gtrsim 4R_\oplus$), low mass ($M \lesssim 6M_\oplus$) planets—but only if they formed at large orbital distances and migrated inward, unlike their more sedentary super-Earth brethren. The outer disk is more conducive to atmospheric accretion because it is colder. Colder gas is less opaque and helps dust-free atmospheres cool and amass faster. For super-puffs to migrate inward by gas disk torques, they must form in a nebula that is not too depleted; the formation of super-puff cores pre-dates the coagulation of super-Earth cores. Super-puff cores may have emerged as isolation masses at large stellocentric distances beyond the ice line. We might expect to find water absorption features in the transmission spectra of super-puffs: infalling icy planetesimals and the erosion of water-rich cores can pollute super-puff envelopes. Our proposal that super-puffs form at distances $\gtrsim$1 AU and migrate inward to their current locations also leads us to expect that super-puffs may be preferentially part of mean-motion resonant chains. Kepler-51 and Kepler-79 are candidate examples (Jontof-Hutter et al. 2014; Masuda 2014). In particular, as one moves outward along a resonant chain, one should find increasingly puffy planets.

Migration of super-puffs (but not super-Earths) may explain why planet masses and by extension bulk densities obtained from transit-timing variations (TTVs) are systematically low compared to those inferred from radial velocity surveys (Jontof-Hutter et al. 2014; Weiss & Marcy 2014, Steffen 2015; Wolfgang et al. 2015). Tightly spaced multi-planet systems situated near mean-motion resonances are the most amenable to TTV analyses. It may therefore be that TTVs are strongest for super-puffs, as we expect to find such objects chained to resonances. Planet formation simulations also show that puffier planets are more tightly packed (Dawson et al. 2015b), further amplifying their TTVs and biasing TTV studies to select for especially low density objects.

### 5.1. Future Directions

In this series of three papers, we have detailed some of the factors relevant for how planets accrete gas from their parent disks and quantified their primordial GCRs. We close now by taking a step back and looking at the broader canvas of issues —what outstanding theoretical questions need to be answered to mature the theory of core nucleation, and how the theory fares against observations.

#### 5.1.1. 3D Hydrodynamics

Our one-dimensional (1D) calculation assumes that accretion flows onto solid cores are spherically symmetric. Three-dimensional (3D) numerical studies show a more complicated flow geometry: cores tend to accrete gas along the poles and expel some fraction of that gas along the equator (e.g., D'Angelo & Bodenheimer 2013; Fung et al. 2015; Ormel et al. 2015). How much 3D hydrodynamics and anisotropies impact gas accretion rates is unclear. Isothermal 3D simulations (Fung et al. 2015; Ormel et al. 2015) find no bound atmosphere; material continuously cycles into and out of the Hill or Bondi sphere. By contrast, 3D simulations that solve the full energy equation with radiative cooling (D'Angelo & Bodenheimer 2013) find not only bound atmospheres but also gas

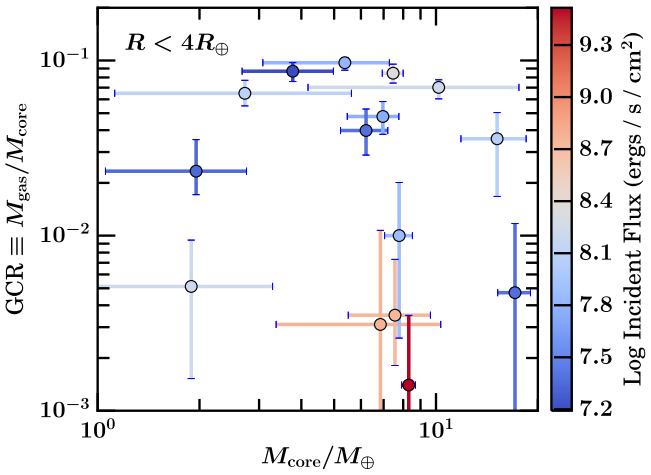


**Figure 8.** Gas-to-core mass ratios (GCRs) vs. core mass (data taken from Table 7 of Lopez & Fortney 2014). The published errors in GCR (a.k.a. envelope fraction) for GJ 1214b, Kepler-11b, 55 Cnc e, Kepler-20c, Kepler-18b, Kepler-68b, and HD 97658b are inaccurate (E. Lopez & J. Fortney 2015, private communication). For these objects, we used uncertainties re-calculated by the authors. The expectation from core accretion theory is that more massive cores should achieve greater gas envelope fractions—all other factors being equal. From the large scatter in this figure, it appears that all other factors are not equal. Up to ~6 $M_\oplus$, GCR increases with $M_{\rm core}$. But at $M_{\rm core} \sim$ 6–8$M_\oplus$, GCR varies across two decades at nearly fixed core mass; the variation appears correlated with incident stellar flux (color shading) and points to the influence of photoevaporative erosion. At $M_{\rm core} > 10\ M_\oplus$, GCRs appear paradoxically to decrease with increasing $M_{\rm core}$. This unexpected behavior might arise because core formation times lengthen with increasing core mass; the most massive cores might take so long to coagulate that by the time they appear, their parent gas disks have long departed.

accretion rates that are comparable to those calculated in 1D. While the results of D'Angelo & Bodenheimer (2013) support 1D studies like ours, their calculations are performed at ~5 AU where 3D effects may be muted because the disk scale height there is safely larger than the planet radius. Future 3D investigations should focus on smaller orbital distances and isolate the effects of thermodynamics: adiabatic simulations should be compared against isothermal simulations and finally against calculations including radiative cooling.

#### 5.1.2. Correlation between Core Mass and Envelope Mass

More massive cores should accrete more massive atmospheres. In Figure 8, drawn from models of planetary interiors by Lopez & Fortney (2014), we examine whether this simple expectation is borne out. It might be, for $M_{\rm core} \lesssim 6M_\oplus$. But for $M_{\rm core} \gtrsim 6\ M_\oplus$, the record of nebular accretion is hard to read. A striking feature in Figure 8 is the large scatter in GCR, spanning two orders of magnitude, within a narrow range of $M_{\rm core} \sim$ 6–8$M_\oplus$. By further color-coding these data by incident stellar flux, we observe that smaller GCRs correlate with larger irradiances, and deduce that evaporative winds powered by stellar irradiation may have eroded GCRs (e.g., Lopez & Fortney 2013; Owen & Wu 2013). The data are scant and hardest to interpret for $M_{\rm core} > 10\ M_\oplus$; here the largest mass cores happen to be the least irradiated yet have the smallest GCRs. Perhaps core formation time is the "hidden variable": if the most massive cores take longer than the gas disk lifetime to coagulate, they will fail to acquire massive atmospheres. Core assembly times can vary by orders of magnitude, depending exponentially on the core mass and the solid surface density of the parent disk (e.g., Dawson et al. 2015a).

#### 5.1.3. Super-Earths versus Jupiters: Trends with Orbital Distance and Host Stellar Type

Our expectation that puffier planets form more easily at larger orbital distances may be tested in individual multi-planet systems. Among the planets with both radii and mass measurements (Masuda 2014; Weiss & Marcy 2014; Jontof-Hutter et al. 2015), we identify five out of nine systems with more than three transiting planets that follow the predicted trend of decreasing bulk density with increasing orbital period: Kepler-20 (Gautier et al. 2012), Kepler-37 (Marcy et al. 2014), Kepler-79 (Jontof-Hutter et al. 2014), Kepler-102 (Marcy et al. 2014), and Kepler-138 (Jontof-Hutter et al. 2015). Of the remaining four systems, three are consistent with the above density trend within errors. The effects of photoevaporative erosion (Owen & Wu 2013) and observational bias (long periods select for larger and presumably puffier planets in transit searches) need to be subtracted off to more cleanly test our theory of atmospheric accretion.

Around FGK stars probed by radial velocity surveys, Jupiters are known to exist preferentially at large orbital distances (e.g., Cumming et al. 2008). It is tempting to ascribe the observed rapid rise in gas giant occurrence rate at ~1 AU to the water ice line in protoplanetary disks. Just outside the water condensation front, the disk's surface density in solids is boosted by ice so that cores massive enough to undergo runaway gas accretion coagulate more quickly, within the gas disk lifetime. Water also accelerates nebular accretion of atmospheres, by virtue of its high mean molecular weight and chemical potential (see footnote 11).

Whether the rise in the gas-giant frequency at ~1 AU coincides with a fall in the super-Earth frequency at that same distance is unclear. Such a fall would signal the transformation of super-Earth cores into Jupiters and would provide strong support for the theory of core accretion. In Paper I (Section 5), we pointed to some data for FGK stars in Fressin et al. (2013) that hinted at such a fall (see also Dong & Zhu 2013; Burke et al. 2015). But the situation is too early to call. It may be instead that the occurrence rate of super-Earths is roughly flat with orbital distance—that super-Earths are truly ubiquitous—as appears to be the case for M stars, as revealed by microlensing (e.g., Gould et al. 2010; Sumi et al. 2010; Cassan et al. 2012; Clanton & Gaudi 2014, 2015) and transit surveys (Dressing & Charbonneau 2015). These same studies indicate that M stars are less likely to host gas giants than FGK stars (see also Bonfils et al. 2013).

Perhaps the simplest picture we can paint with the data and theory currently in hand is that most stars in the universe are born with disks having solid surface densities that are neither too "low" nor too "high." The higher the solid surface density, the faster the coagulation of rocky cores (Dawson et al. 2015a). Most disks have "medium" solid surface densities in the sense that they spawn super-Earth cores near the tail-end of the gas lifetime (scenario b)—neither so fast that cores are birthed into gas-rich environments to become Jupiters, nor so slow that they fail to acquire any atmosphere at all because the parent gas disk has completely dissipated. We have seen in this paper that this middle ground is enormous and presents no fine-tuning problems. A minority of FGK stars—about ~10% (Cumming et al. 2008)—have disk surface densities just high enough to spawn Jupiters, and then only with the added boost from the ice line at ~1 AU. In this picture, there should be a corresponding drop in the occurrence rates of super-Earths at that distance around FGK

stars. As for M dwarf disks, we posit that their surface densities are systematically lower than those of their FGK counterparts (see also Laughlin et al. 2004; Andrews et al. 2013; cf. Kornet et al. 2006), so much so that they almost never produce gas giants, but instead make super-Earths everywhere. The unifying theme in this rough sketch is disk solid surface density and its decisive impact on planet demographics.

Our high-$Z$ analysis was made possible by Jason Ferguson, who generously calculated all the opacity tables for $\log T$ (K) $> 2.7$. We thank Heather Knutson, Chris Ormel, James Owen, and an anonymous referee for careful readings of our manuscript that led to substantive improvements, and Gennaro D'Angelo, Rebekah Dawson, Jonathan Fortney, Jeffrey Fung, Eric Lopez, Ruth Murray-Clay, Sergei Nayakshin, and Yanqin Wu for helpful discussions. We are also grateful to Daniel Fabrycky and Hilke Schlichting for motivating us to consider the formation of super-puffs; David Bennett, Christian Clanton, and Scott Gaudi for educating us about planet occurrence rates around M stars as measured by microlensing surveys; and Jeff Cuzzi and Jack Lissauer for prompting us to revisit the assumption of dusty atmospheres.

E.J.L. is supported in part by the Natural Sciences and Engineering Research Council of Canada under PGS D3 and the Berkeley Fellowship. E.C. acknowledges support from grants AST-0909210 and AST-1411954 awarded by the National Science Foundation, NASA Origins grant NNX13AI57G, and *Hubble Space Telescope* grant *HST*-AR-12823.001-A.

Numerical calculations were performed on the SAVIO computational cluster resource provided by the Berkeley Research Computing program at the University of California Berkeley, supported by the UC Chancellor, the UC Berkeley Vice Chancellor for Research, and Berkeley's Chief Information Officer.

## REFERENCES

Agnor, C. B., & Ward, W. R. 2002, ApJ, 567, 579
Alexander, R., Pascucci, I., Andrews, S., Armitage, P., & Cieza, L. 2014, in Protoplanets and Protostars VI, ed. H. Beuther et al. (Tuscon, AZ: Univ. Arizona Press), 475
Andrews, S. M., Rosenfeld, K. A., Kraus, A. L., & Wilner, D. J. 2013, ApJ, 771, 129
Batalha, N. M., Rowe, J. F., Bryson, S. T., et al. 2013, ApJS, 204, 24
Biddle, L. I., Pearson, K. A., Crossfield, I. J. M., et al. 2014, MNRAS, 443, 1810
Blum, J., & Wurm, G. 2000, Icar, 143, 138
Bonfils, X., Delfosse, X., Udry, S., et al. 2013, A&A, 549, A109
Burke, C. J., Christiansen, J. L., Mullally, F., et al. 2015, ApJ, 809, 8
Casassus, S., Marino, S., Perez, S., et al. 2015, ApJ, 811, 92
Cassan, A., Kubas, D., Beaulieu, J.-P., et al. 2012, Natur, 481, 167
Chambers, J. E., Wetherill, G. W., & Boss, A. P. 1996, Icar, 119, 261
Chiang, E., & Laughlin, G. 2013, MNRAS, 431, 3444
Chiang, E., & Murray-Clay, R. 2007, NatPh, 3, 604
Clanton, C., & Gaudi, B. S. 2014, ApJ, 791, 91
Clanton, C., & Gaudi, B. S. 2015, arXiv:1508.04434
Clarke, C. J., Gendrin, A., & Sotomayor, M. 2001, MNRAS, 328, 485
Crossfield, I. J. M., Barman, T., Hansen, B. M. S., & Howard, A. W. 2013, A&A, 559, A33
Cumming, A., Butler, R. P., Marcy, G. W., et al. 2008, PASP, 120, 531
D'Alessio, P., Calvet, N., & Hartmann, L. 2001, ApJ, 553, 321
D'Angelo, G., & Bodenheimer, P. 2013, ApJ, 778, 77
Dawson, R., Chiang, E., & Lee, E. 2015a, MNRAS, 453, 1471
Dawson, R. I., Lee, E. J., & Chiang, E. 2015b, arXiv:1512.04951
Dong, S., & Zhu, Z. 2013, ApJ, 778, 53
Drake, J. J., Ercolano, B., Flaccomio, E., & Micela, G. 2009, ApJL, 699, L35
Dressing, C. D., & Charbonneau, D. 2015, ApJ, 807, 45
Duffell, P. C., & Chiang, E. 2015, ApJ, 812, 94
Espaillat, C., Muzerolle, J., Najita, J., et al. 2014, in Protostars and Planets VI, ed. H. Beuther et al. (Tuscon, AZ: Univ. of Arizona Press), 497
Ferguson, J. W., Alexander, D. R., Allard, F., et al. 2005, ApJ, 623, 585
Ford, E. B., & Chiang, E. I. 2007, ApJ, 661, 602
Fraine, J., Deming, D., Benneke, B., et al. 2014, Natur, 513, 526
Fressin, F., Torres, G., Charbonneau, D., et al. 2013, ApJ, 766, 81
Fung, J., Artymowicz, P., & Wu, Y. 2015, arXiv:1505.03152
Gautier, T. N., III, Charbonneau, D., Rowe, J. F., et al. 2012, ApJ, 749, 15
Goldreich, P., Lithwick, Y., & Sari, R. 2004, ARA&A, 42, 549
Goldreich, P., & Sari, R. 2003, ApJ, 585, 1024
Gould, A., Dong, S., Gaudi, B. S., et al. 2010, ApJ, 720, 1073
Hadden, S., & Lithwick, Y. 2014, ApJ, 787, 80
Hori, Y., & Ikoma, M. 2011, MNRAS, 416, 1419
Howard, A. W., Marcy, G. W., Johnson, J. A., et al. 2010, Sci, 330, 653
Ikoma, M., & Hori, Y. 2012, ApJ, 753, 66
Ikoma, M., Nakazawa, K., & Emori, H. 2000, ApJ, 537, 1013
Inamdar, N. K., & Schlichting, H. E. 2015, MNRAS, 448, 1751
Iwasaki, K., Tanaka, H., Nakazawa, K., & Hiroyuki, E. 2001, PASJ, 53, 321
Jontof-Hutter, D., Lissauer, J. J., Rowe, J. F., & Fabrycky, D. C. 2014, ApJ, 785, 15
Jontof-Hutter, D., Rowe, J. F., Lissauer, J. J., Fabrycky, D. C., & Ford, E. B. 2015, Natur, 522, 321
Knutson, H. A., Benneke, B., Deming, D., & Homeier, D. 2014, Natur, 505, 66
Kominami, J., & Ida, S. 2002, Icar, 157, 43
Kornet, K., Wolf, S., & Różyczka, M. 2006, A&A, 458, 661
Kreidberg, L., Bean, J. L., Désert, J.-M., et al. 2014, Natur, 505, 69
Laughlin, G., Bodenheimer, P., & Adams, F. C. 2004, ApJL, 612, L73
Lee, E. J., & Chiang, E. 2015, ApJ, 811, 41
Lee, E. J., Chiang, E., & Ormel, C. W. 2014, ApJ, 797, 95
Line, M., & Parmentier, V. 2015, arXiv:1511.09443
Lopez, E. D., & Fortney, J. J. 2013, ApJ, 776, 2
Lopez, E. D., & Fortney, J. J. 2014, ApJ, 792, 1
Mamajek, E. E. 2009, in AIP Conf. Ser. 1158, Exoplanets and Disks: Their Formation and Diversity, ed. T. Usuda, M. Tamura & M. Ishii (Melville, NY: AIP), 3
Marcy, G. W., Isaacson, H., Howard, A. W., et al. 2014, ApJS, 210, 20
Masuda, K. 2014, ApJ, 783, 53
Mizuno, H. 1980, PThPh, 64, 544
Mordasini, C., Klahr, H., Alibert, Y., Miller, N., & Henning, T. 2014, A&A, 566, A141
Morley, C. V., Fortney, J. J., Kempton, E. M.-R., et al. 2013, ApJ, 775, 33
Nettelmann, N., Fortney, J. J., Kramm, U., & Redmer, R. 2011, ApJ, 733, 2
Ogihara, M., Ida, S., & Morbidelli, A. 2007, Icar, 188, 522
Ormel, C. W. 2014, ApJL, 789, L18
Ormel, C. W., Shi, J.-M., & Kuiper, R. 2015, MNRAS, 447, 3512
Owen, J. E., Clarke, C. J., & Ercolano, B. 2012, MNRAS, 422, 1880
Owen, J. E., Ercolano, B., & Clarke, C. J. 2011, MNRAS, 412, 13
Owen, J. E., & Wu, Y. 2013, ApJ, 775, 105
Papaloizou, J. C. B., & Larwood, J. D. 2000, MNRAS, 315, 823
Petigura, E. A., Marcy, G. W., & Howard, A. W. 2013, ApJ, 770, 69
Piso, A.-M. A., & Youdin, A. N. 2014, ApJ, 786, 21
Piso, A.-M. A., Youdin, A. N., & Murray-Clay, R. A. 2015, ApJ, 800, 82
Pollack, J. B., Hubickyj, O., Bodenheimer, P., et al. 1996, Icar, 124, 62
Pu, B., & Wu, Y. 2015, ApJ, 807, 44
Rogers, L. A., & Seager, S. 2010a, ApJ, 712, 974
Rogers, L. A., & Seager, S. 2010b, ApJ, 716, 1208
Rosenfeld, K. A., Chiang, E., & Andrews, S. M. 2014, ApJ, 782, 62
Rowe, J. F., Bryson, S. T., Marcy, G. W., et al. 2014, ApJ, 784, 45
Safronov, V. S. 1972, Evolution of the Protoplanetary Cloud and Formation of the Earth and Planets (Jerusalem: Keter Publishing House)
Steffen, J. H. 2015, arXiv:1510.04750
Steffen, J. H., Batalha, N. M., Borucki, W. J., et al. 2010, ApJ, 725, 1226
Steffen, J. H., Fabrycky, D. C., Agol, E., et al. 2013, MNRAS, 428, 1077
Stevenson, D. J. 1982, P&SS, 30, 755
Stevenson, D. J. 1984, in Lunar and Planetary Science Conf., Lunar and Planetary Inst. Technical Report, Vol. 15, 822
Sumi, T., Bennett, D. P., Bond, I. A., et al. 2010, ApJ, 710, 1641
Van Eylen, V., & Albrecht, S. 2015, ApJ, 808, 126
Venturini, J., Alibert, Y., Benz, W., & Ikoma, M. 2015, A&A, 576, A114
Weiss, L. M., & Marcy, G. W. 2014, ApJL, 783, L6
Windmark, F., Birnstiel, T., Ormel, C. W., & Dullemond, C. P. 2012, A&A, 544, L16
Wolfgang, A., & Lopez, E. 2015, ApJ, 806, 183
Wolfgang, A., Rogers, L. A., & Ford, E. B. 2015, arXiv:1504.07557
Wu, Y., & Lithwick, Y. 2013, ApJ, 772, 74
Zhou, J.-L., Lin, D. N. C., & Sun, Y.-S. 2007, ApJ, 666, 423